# Stabilizing time-shift estimates in coda wave interferometry with the dynamic time warping method

*T. Dylan Mikesell*, Alison Malcolm and Di Yang, Earth Resources Laboratory, MIT; Matt M. Haney, Alaska Volcano Observatory, USGS*

## SUMMARY

Accurate time-shift estimation between arrivals in two seismic traces before and after a small velocity change is crucial for estimating the location and amplitude of velocity the change. Windowed crosscorrelation and trace stretching are two techniques commonly used to estimate local time shifts in multiply scattered coda signals. These methods both suffer when the induced changes in the scattered wavefield are not simple shifts. Cycle skipping is an example of one such obstacle that neither method is able to overcome. A common approach to mitigate such problems is to choose only part of the coda to analyze. In the work presented here, we implement Dynamic Time Warping (DTW) to search for the time shift at each time sample that globally minimizes the misfit between two seismic traces. We show that DTW is not as susceptible to errors in time-shift estimates caused by cycle skipping or disappearance of coda phases due to changes in scattering. Our approach provides a new tool to estimate small time shifts in coda and has wide application across all disciplines of seismic monitoring with coda waves.

## INTRODUCTION

Unraveling the multiply scattered wavefield, commonly called coda, in the Earth is a difficult task. Over decades seismologists have developed different approaches to understand and use the coda signal, e.g. to determine earthquake magnitude (see Chapter 3.2 in Sato et al., 2012, and references therein). Numerous authors have demonstrated the use of coda waves to monitor small velocity changes in different geologic settings (see Poupinet et al., 2008, and references therein). The reason that coda waves are often used is because they travel through the subsurface over larger distances than the ballistic waves. Therefore, coda waves sample the medium much more; in effect making them very sensitive to the velocity structure. The difficulty however, comes in using coda waves to understand the spatial distribution of the velocity heterogeneity.

Researchers across many fields have suggested ways to analyze and interpret complex coda wave signals. In seismology the active doublet (Poupinet et al., 1984; Roberts et al., 1992) and coda wave interferometry (CWI) (Snieder, 2006) methods are approaches to quantify small velocity changes using coda waves. The methods are based on the assumption that a velocity change induces measurable phase shifts in the coda. Pacheco and Snieder (2005) developed a framework for the spatial sensitivity of coda time shifts ($\Delta t$) to velocity perturbations ($\Delta V$) using a diffusion based kernel to represent the coda wavefield with time:

$$\frac{\Delta t}{t} = -K(\mathbf{x}_s, \mathbf{x}_r, t)\frac{\Delta V}{V}, \tag{1}$$

where the kernel ($K$) is a function of the source and receiver positions $\mathbf{x}_s$ and $\mathbf{x}_r$, respectively. The time shifts can be estimated using windowed crosscorrelation or crosscoherency (e.g. Poupinet et al., 1984; Grêt et al., 2006; Haney et al., 2009) or trace stretching (e.g. Sens-Schönfelder and Wegler, 2006; Hadziioannou et al., 2009), and the kernels can also be derived using radiative transfer theory (e.g. Planès et al., 2014).

If only isolated parts of the medium velocity are perturbed, then only isolated parts of the coda should change (Pacheco and Snieder, 2006). For example, if only a single reservoir velocity changes, then only parts of the coda that contain waves sampling this reservoir will change (e.g. Khatiwada et al., 2012). When the velocity change $\Delta V$ is not homogeneous, windowed crosscorrelation is known to under estimate $\Delta t$, especially at large lag times. This underestimation can be due to the crosscorrelation detecting the lag time that maximizes the correlation within the window, which may contain waves that did not sample the velocity change. Another cause is cycle skipping due to the time shift exceeding the dominant period (e.g. McGuire et al., 2012) or due to changes in the waveform caused by changes in scattering.

Hale (2013) demonstrates the advantages of the Dynamic Time Warping (DTW) method over crosscorrelation to measure variations in time-lapse seismic images. Here we compare the DTW estimated shifts to time shifts estimated by the windowed crosscorrelation method. DTW has been shown to out perform crosscorrelation when time and frequency shifts are nonlinear and strong noise is present (Hale, 2013). Recent examples of DTW use in the seismic exploration industry can be found in well-tie experiments (e.g. Muñoz and Hale, 2012; Herrera and van der Baan, 2012). With this in mind, we investigate the use of DTW to measure small delays in coda wave signals caused by isolated velocity perturbations. Using DTW we can impose constraints on how rapidly shifts vary with time to suppress cycle skipping, but we need not constrain the linearity of these shifts. This is an advantage over current methods.

## THEORY

As evident by equation 1, if the $\Delta t$ value is not correctly estimated, the corresponding velocity perturbation $\Delta V$ is not correctly estimated, even if an accurate kernel is available. Dynamic time warping (DTW) is a nonlinear optimization approach (Sakoe and Chiba, 1978) which we use to measure time shifts between coda arrivals before and after a velocity change has occurred in the subsurface. We implement DTW following Hale (2013) and quantify the magnitude of time shifts in coda waves. Below we give a short description of the method; however, we suggest the reader see Müller (2007) or Hale (2013) for a more complete description of the DTW algorithm and the underlying details and assumptions.

Consider the seismogram $g(t_i)$, where $t_i$ is the time sample index. If we apply a time-varying shift $s(t_i)$ to $g(t_i)$ then we obtain a second seismogram $f(t_i) \approx g(t_i + s(t_i))$, which is approximately the time-shifted version of the original $g(t_i)$. Following Hale (2013), we define the error function

$$e(t_i, t_l) = (f(t_i) - g(t_i + t_l))^2, \quad (2)$$

where $t_l$ is a lag time, defined by the user. The first step in DTW is to compute the error function for all possible times $t_i$ and for a range of lags $t_l$. The lags can increment at a fraction of the sample interval while the maximum lag can be a fraction of the total trace length. The next step is to search, in both the forward and backward time directions, through this error function, accumulating errors. The final step is to find the minimum error (warping) path, via optimization, which should result in a function close to the original shift $s(t_i)$. Setting the lag increment defines the maximum time jump from one sample to the next, in essence a smoothness constraint (see Hale, 2013, *Limiting strain* section for complete details). This constraint is why DTW is less sensitive to cycle skipping.

Dynamic time warping optimizes the misfit between each sample in the two traces. Therefore, if only a few arrivals in the coda have sampled the velocity change, the estimated time shifts are nonlinear. In the *stretching* method used in many coda wave monitoring studies (e.g. Hadziioannou et al., 2011), $s(t_i) = \varepsilon * t_i$, where $\varepsilon = \Delta V/V$ is the stretching coefficient. Right away, we see the linearity constraint imposed in the stretching method and note that in DTW we do not have this constraint.

## A NUMERICAL EXPERIMENT

We investigate the use of DTW to estimate time shifts in the coda using a 2-dimensional (2D) acoustic model with a random Gaussian slowness distribution. We use the 2D background velocity model shown in Figure 1(a). The inner circle velocity is 6 km/s and remains constant throughout all of the experiments. We vary the outer circle velocity from -3% to +3% of the inner circle velocity at 1% increments (i.e., $\Delta V$ = -180, -120, -60, 0, +60, +120, +180 m/s, respectively). In Figure 1(a) we show the +1% velocity model. The model is 32 km $\times$ 32 km with absorbing boundaries. The grid spacing is 20 m in the simulations.

We use the SeisUnix 2D finite-difference code *sufdmod2* to model the acoustic wavefield for 10 s after the source impact. The source is a 10 Hz (center frequency) Ricker wavelet; therefore, at 6 km/s the dominant wavelength is 600 m. After simulation, we resample the data to an interval of 1 ms. The receiver (gray reverse triangle in Figure 1(a)) and source (gray star in Figure 1(b)) are co-located at the center of model. To suppress reflections from the inner-outer boundary we taper the background velocity model from the inner to the outer circle. The taper width is 2 km and starts 6 km from the center of the model.

To create the multiply scattered coda wavefield, we generate a random Gaussian slowness distribution and overlay this on the various background velocity models. The random slowness model is shown in Figure 1(b) as velocity. The average size of the perturbations are on the order of 400 m. For each of the various background velocity models we show the individual waveforms in Figure 2(a). The wiggle traces are underlain by the grey boxes in certain places to help visualize the wavefield changes in the different models. For instance, looking at arrivals around 8 and 9 s, we see the appearance or disappearance of coda arrivals, as well as changes in the frequency of arrivals

## TIME-SHIFT ESTIMATION

We compare the DTW method to the windowed crosscorrelation method. The window length is 0.8 s – roughly $8T$, where $T = 0.1$ s is the dominant period. For the reference trace, to which we compare all other traces, we use the model that does not differ across the inner and outer boundary (i.e. $\Delta V = 0$, gray trace in Figure 2(a)). For each of the different traces in Figure 2(a), we slide the crosscorrelation window 1 sample at a time, recording the maximum correlation coefficient and the lag at that maximum correlation. The correlation coefficients and lag times are plotted in Figure 2(b) and 2(c), respectively.

For each model, the inner background velocity does not change. Therefore, we do not expect any change in the waveforms until after the time when waves could have reached the inner-outer boundary and returned to the receiver. This time is approximately 2.5 s and the correlation coefficients in Figure 2(b) demonstrate this; the traces are identical up to $\sim 2.5$ s, after which the correlation coefficient begins to decrease. Note that the models with larger velocity perturbations start to lose correlation more rapidly than those with smaller velocity perturbations.

The time shifts estimated by the crosscorrelation method in Figure 2(c) also show that $\Delta t = 0$ before 2.5 s and starts to decrease or increase more-or-less linearly until the first cycle skip occurs. The first cycle skip time is different for each trace, but the skipping begins when $\Delta t$ approaches 1 period, $T = 0.1$ s. Therefore, the skipping begins earlier for the larger velocity perturbation models (e.g., the blue line in Figure 2(c) for $\Delta V$ = -180 m/s).

Once cycle skipping occurs, the correlation coefficients start to decay and oscillate, and it is difficult to trust the $\Delta t$ estimates based correlation coefficients, even as they overcome the cycle skipping at later times. It is worth noting that when the crosscorrelation window is $8T$, the cycle skipping remains a problem and only worsens as the window size decreases. This is because the correlation function only identifies the *local* lag time between the two windows and is sensitive to changes in scattering (e.g. Larose et al., 2010). We can directly see this sensitivity by considering the $\Delta t$ estimates around 8 s for the $\Delta V = 180$ m/s trace. We see that the arrival just after 8 s in the $\Delta V = 0$ trace disappears in the $\Delta V = 180$ m/s trace. This causes a cycle skip in the $\Delta t$ estimate (Figure 2(c)).

We apply DTW to the same reference and perturbed traces to estimate time shifts (Figure 2(d)). The maximum possible lag is 0.5 s and the lag interval is 0.1 ms. Right away we see that cycle skipping is no longer a problem. This is due to search-

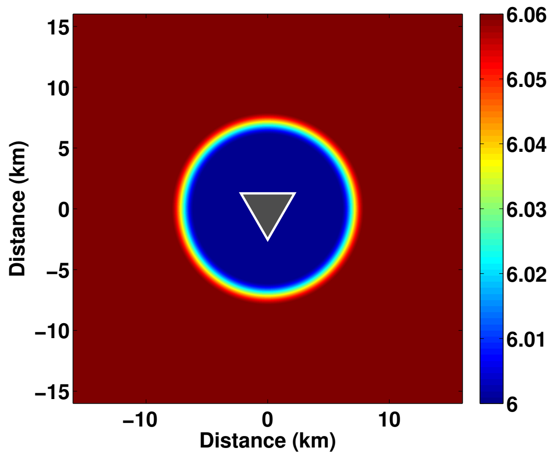


(a)

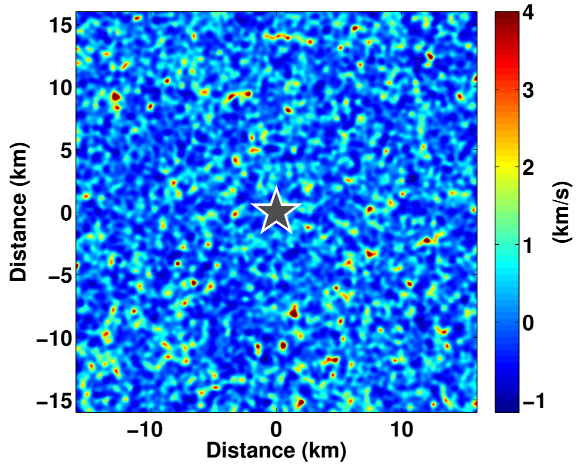


(b)

Figure 1: (a) Acoustic background velocity model with outer velocity equal to +1% of inner velocity; receiver indicated by the gray reverse triangle. (b) Random Gaussian velocity perturbation model that is overlain on the background model; acoustic source indicated by the gray star.

ing in the forward and backward directions for the set of lags that give minimum misfit to the entire trace, not a window. We also note that the DTW time shift estimates show more small scale variation compared to the windowed crosscorrelation. This is due to the windowed crosscorrelation averaging time shifts within the 0.8 s window.

## DISCUSSION

There is no correlation coefficient to go along with the $\Delta t$ estimates in Figure2(d); but as discussed above, these $\Delta t$ estimates globally minimize the misfit between the two traces. Studies have been made to characterize the accuracy of estimated $\Delta t$ values from the various methods (e.g. Clarke et al., 2011). The next step in our analysis will be to create a method to quantify the accuracy of $\Delta t$ picks from DTW.

Beyond using $\Delta t$ estimates, researchers are also beginning to use the windowed crosscorrelation coefficient itself as a complementary data (Larose et al., 2010; Rossetto et al., 2011). They use the decoherence, defined as $1.0 - CC$, where $CC$ is the correlation coefficient, to show that imaging isolated velocity perturbations using coda waves is possible. Obermann et al. (2013a) show that the *stretching* $\Delta t$ measurements combined with the decoherence measurement is well suited for interpreting coda in the Earth.

Interestingly, the decoherence method entails using the maximum correlation coefficient at the time lag $\Delta t$. Therefore, even this complementary data hinges on our ability to find the right $\Delta t$. Furthermore, Obermann et al. (2013b) showed with synthetic examples that the early coda is dominated by surface waves while the later coda is comprised mostly of body waves for a source and receiver at the surface. These different waves travel at different velocities; therefore we should not expect a linear increase in $\Delta t$ as imposed by the *stretching* method. Dynamic time warping does not impose constraints on the linearity of shifts, only on the slope of the $\Delta t$ function. Therefore, DTW has the ability to more accurately represent the time variant $\Delta t$ as demonstrated in Figure 2(d).

## CONCLUSION

We apply the Dynamic Time Warping (DTW) method to two seismic traces in order to estimate time shifts in the multiply scattered coda wavefield. These time shifts are caused by perturbations in the background velocity of a random Gaussian slowness model. We compare the DTW method to the often used windowed crosscorrelation method. The velocity model perturbations range from -3% to +3% at a $\pm 1\%$ interval. We show that the DTW method is considerably more stable than crosscorrelation, even when the correlation window length is 8 times the period. In all of the tested velocity models, the DTW $\Delta t$ estimate does not cycle skip when we set the lag interval to one-tenth the sample interval. Furthermore, the DTW estimate shows more fine scale structure than the crosscorrelation estimate. This is because the crosscorrelation averages over the entire window. This new application has the potential for widespread use across all disciplines using coda waves to monitor changes in velocity over time.

## ACKNOWLEDGMENTS

We are grateful to Oleg Poliannikov for providing the code to generate the random Gaussian slowness model, as well as the developers of SeisUnix, which we used for the finite difference modeling in this work. T. D. M. thanks Kasper van Wijk and Guust Nolet for useful discussions about changes in coda waves and acknowledges financial support from the National Science Foundation under Award No. 1144883.

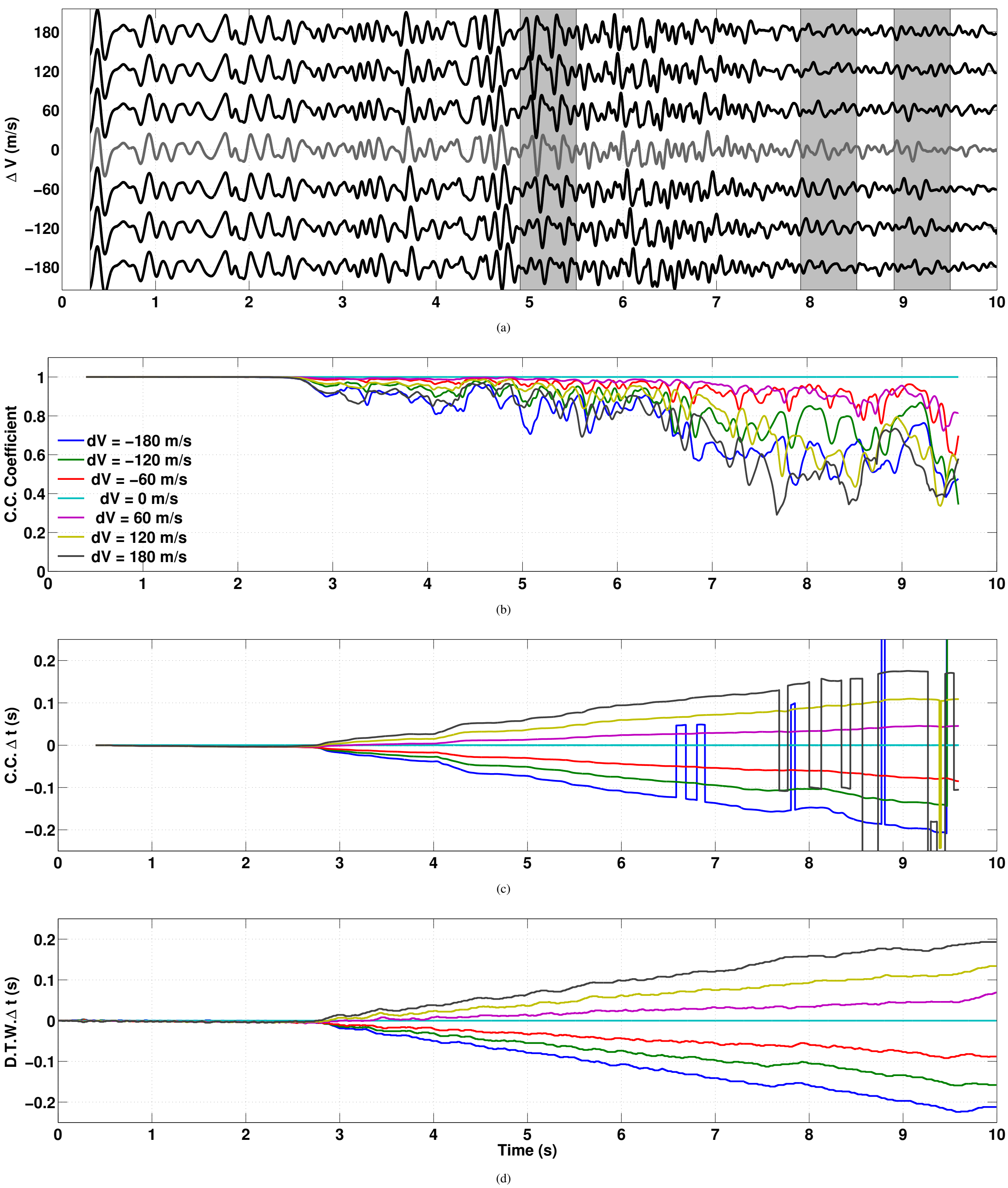


Figure 2: (a) Seismic wiggle traces; the large amplitude direct wave arrival ($t < 0.25$ s) is muted because it has significantly larger amplitude than the scattered waves. Underlying grey boxes indicate notable changes in the coda waveforms, not just time shifts. From bottom to top, the outer velocity for each trace changes by -180, -120, -60, 0, +60, +120, & +180 m/s, respectively. The middle gray trace ($\Delta V = 0$) is the reference trace to which all other traces are correlated or warped. (b) Correlation coefficients from the sliding window crosscorrelation method; the window length is 0.8 s. (c) $\Delta t$ estimates from sliding window crosscorrelation. (d) $\Delta t$ estimates from dynamic time warping. The maximum lag is set to 0.5 s and the lag interval is 0.1 ms.

## REFERENCES

Clarke, D., L. Zaccarelli, N. M. Shapiro, and F. Brenguier, 2011, Assessment of resolution and accuracy of the Moving Window Cross Spectral technique for monitoring crustal temporal variations using ambient seismic noise: Geophysical Journal International, **186**, 867–882.

Grêt, A., R. Snieder, and J. Scales, 2006, Time-lapse monitoring of rock properties with coda wave interferometry: Journal of Geophysical Research, **111**, B03305.

Hadziioannou, C., E. Larose, A. Baig, P. Roux, and M. Campillo, 2011, Improving temporal resolution in ambient noise monitoring of seismic wave speed: Journal of Geophysical Research, **116**, B07304.

Hadziioannou, C., E. Larose, O. Coutant, P. Roux, and M. Campillo, 2009, Stability of monitoring weak changes in multiply scattering media with ambient noise correlation: laboratory experiments: Journal of the Acoustical Society of America, **125**, 3688–95.

Hale, D., 2013, Dynamic warping of seismic images: Geophysics, **78**, S105–S115.

Haney, M. M., K. van Wijk, L. A. Preston, and D. F. Aldridge, 2009, Observation and modeling of source effects in coda wave interferometry at Pavlof volcano: The Leading Edge, 554–560.

Herrera, R. H., and M. van der Baan, 2012, Automated Seismic-to-well Ties?: 74th EAGE Conference & Exhibition, IO31.

Khatiwada, M., L. Adam, M. Morrison, and K. van Wijk, 2012, A feasibility study of time-lapse seismic monitoring of CO2 sequestration in a layered basalt reservoir: Journal of Applied Geophysics, **82**, 145–152.

Larose, E., T. Planès, V. Rossetto, and L. Margerin, 2010, Locating a small change in a multiple scattering environment: Applied Physics Letters, **96**, 204101.

McGuire, J. J., J. A. Collins, P. Gouédard, E. Roland, D. Lizarralde, M. S. Boettcher, M. D. Behn, and R. D. van der Hilst, 2012, Variations in earthquake rupture properties along the Gofar transform fault, East Pacific Rise: Nature Geoscience, **5**, 336–341.

Muñoz, A., and D. Hale, 2012, Automatically tying well logs to seismic data: Technical report, CWP-725, Colorado School of Mines, Golden, CO.

Müller, M., 2007, Information Retrieval for Music and Motion: Springer.

Obermann, A., T. Planès, E. Larose, and M. Campillo, 2013a, Imaging preeruptive and coeruptive structural and mechanical changes of a volcano with ambient seismic noise: Journal of Geophysical Research: Solid Earth, **118**, 1–10.

Obermann, A., T. Planès, E. Larose, C. Sens-Schönfelder, and M. Campillo, 2013b, Depth sensitivity of seismic coda waves to velocity perturbations in an elastic heterogeneous medium: Geophysical Journal International, **194**, 372–382.

Pacheco, C., and R. Snieder, 2005, Time-lapse travel time change of multiply scattered acoustic waves: Journal of the Acoustical Society of America, **118**, 1300–1310.

———, 2006, Time-lapse traveltime change of singly scattered acoustic waves: Geophysical Journal International, **165**, 485–500.

Planès, T., E. Larose, L. Margerin, V. Rossetto, and C. Sens-Schönfelder, 2014, Decorrelation and phase-shift of coda waves induced by local changes: multiple scattering approach and numerical validation: Waves in Random and Complex Media, 1–27.

Poupinet, G., W. L. Ellsworth, and J. Frechet, 1984, Monitoring velocity vartiations in the crust using earthquake doublets: An application to the Calaveras Fault, California: Journal of Geophysical Research, **89**, 5719–5731.

Poupinet, G., J. L. Got, and F. Brenguier, 2008, Chapter 14: Monitoring Temporal Variations of Physical Properties in the Crust by Cross-Correlating the Waveforms of Seismic Doublets: Advances in Geophysics, **50**, 373–399.

Roberts, P. M., W. S. Phillips, and M. C. Fehler, 1992, Development of the active doublet method for measuring small velocity and attenuation changes in solids: Journal of the Acoustical Society of America, **91**, 3291–3302.

Rossetto, V., L. Margerin, T. Planès, and E. Larose, 2011, Locating a weak change using diffuse waves: Theoretical approach and inversion procedure: Journal of Applied Physics, **109**, 034903.

Sakoe, H., and S. Chiba, 1978, Dynamic programming algorithm optimization for spoken word recognition: IEEE Transactions on Acoustics, Speech, and Signal Processing, **ASSP-26**, 43–49.

Sato, H., M. C. Fehler, and T. Maeda, 2012, Seismic wave propagation and scattering in the heterogeneous Earth, 2nd ed.: Springer.

Sens-Schönfelder, C., and U. Wegler, 2006, Passive image interferometry and seasonal variations of seismic velocities at Merapi Volcano, Indonesia: Geophysical Research Letters, **33**.

Snieder, R., 2006, The Theory of Coda Wave Interferometry: Pure and Applied Geophysics, **163**, 455–473.